Published in final edited form as:
J Acoust Soc Am. 2019 March 01; 145(3): 1389. doi:10.1121/1.5093623.

Simulations of the effect of unlinked cochlear-implant automatic gain control and head movement on interaural level differences

Alan W. Archer-Boyd, **Robert P. Carlyon**
MRC Cognition and Brain Sciences Unit, University of Cambridge, 15 Chaucer Rd., Cambridge, CB2 7EF, United Kingdom

Abstract

This study simulated the effect of unlinked automatic gain control (AGC) and head movement on the output levels and resulting ILDs produced by bilateral CI processors. The angular extent and velocity of the head movements were varied in order to observe the interaction between unlinked AGC and head movement. Static, broadband input ILDs were greatly reduced by the high-ratio, slow time-constant AGC used. The size of head-movement-induced dynamic ILDs depended more on the velocity and angular extent of the head movement than on the angular position of the source. The profiles of the dynamic, broadband output ILDs were very different from the dynamic, broadband input ILD profiles. Short-duration, high-velocity head movements resulted in dynamic output ILDs that continued to change after head movement had stopped. Analysis of narrowband, single-channel ILDs showed that static output ILDs were reduced across all frequencies, producing low-frequency ILDs of the opposite sign to the high-frequency ILDs. During head movements, low-frequency and high-frequency ILDs changed with opposite sign. The results showed that the ILDs presented to bilateral CI listeners during head turns were highly distorted by the interaction of the bilateral, unlinked AGC and the level changes induced by head movement.

Keywords

cochlear implants; dynamic-range compression; head movement; interaural level differences

I Introduction

Automatic gain control (AGC) is used both in hearing aids and cochlear implants (CI) to compensate for the reduced dynamic range of hearing compared to that of normal hearing (NH) listeners. In the case of CIs the electrically stimulated dynamic range is only 10-20 dB (Skinner *et al.*, 1997; Zeng and Galvin, 1999; Zeng *et al.*, 2002), compared to the 100 dB in NH. The AGCs used in CIs generally include a slow-acting system, with a low threshold and high compression ratio, combined with a fast-acting system having a higher threshold (known as a “dual-loop compressor”). The fast-acting system acts like a limiter, preventing listeners from being exposed to sudden, loud sounds. The present study investigates the effects of the slow-acting compressor on the inter-aural level differences (ILDs) presented to CI listeners, with particular reference to the combined effects of AGCs and head movements.

Europe PMC Funders Author Manuscripts

We believe that it is particularly important to study these effects in CI listeners for two reasons. First, CI listeners rely almost entirely on ILDs for sound localization in the azimuth; interaural time differences (ITDs) are generally unavailable because the pulses in bilateral processors are not synchronized between the two ears in clinical use (Seeber *et al.*, 2004), and are often poorly processed even in experiments that manipulate ITDs directly (Van Hoesel, 2004). This contrasts with NH listeners who are more likely to use both ILDs and ITDs equally (Bronkhorst, 2000; van Hoesel *et al.*, 2002; van Hoesel and Tyler, 2003; Seeber and Fastl, 2008; van Hoesel *et al.*, 2008). Second, the slow AGC used in CIs has a longer time constant and much higher compression ratio (e.g. 12:1 in devices made by Advanced Bionics Ltd) than that implemented in hearing aids. As we shall argue, this is likely to increase the distortions of ILDs induced by the combination of the AGC and head movement.

AGC has been shown to affect the perceived position of sound sources even for steady sounds presented to NH listeners with static heads, and using a modest compression ratio of 3:1 (Wiggins and Seeber, 2011; Schwartz and Shinn-Cunningham, 2013), although studies involving hearing-impaired listeners show mixed results (Keidser *et al.*, 2006; Musa-Shufani *et al.*, 2006; Hassager *et al.*, 2017). AGC also reduces the size of ILDs available to CI users (Dorman *et al.*, 2014). and have been shown to increase average ILD thresholds from 1.9 to 3.8 dB in eleven post-lingually deaf bilateral Med-El Combi 40+ users (Grantham *et al.*, 2008). Directly stimulated electrode pairs can result in ILD thresholds that are comparable to that of NH listeners (Laback *et al.*, 2004), and can in some cases be below the smallest step size available (e.g. 0.17 dB in CIs made by Cochlear Ltd.; van Hoesel and Tyler, 2003). Because CIs usually incorporate high-pass pre-emphasis filters prior to a single-channel broadband AGC, the gain applied by the AGC is dominated by the high-frequency part of the input spectrum. This, combined with high compression ratios and the head-shadow effect (essentially a low-pass filter at the contralateral ear) can induce ILDs at low frequencies that are inverted in sign relative to the ‘true’ ILD (Dorman *et al.*, 2014).

Head movements have recently received more attention in auditory science (e.g. Veugen *et al.*, 2017; Agterberg, 2018; Archer-Boyd *et al.*, 2018; Ege *et al.*, 2018). They are an important cue for resolving front-back confusions in NH listeners(Brimijoin and Akeroyd, 2012), and CI listeners (Goman, 2014; Mueller *et al.*, 2014; Pastore *et al.*, 2018). For example, Pastore *et al.* (2018) recently reported that CI listeners were able to utilize head movements to resolve front-back confusions when listening through bilateral unlinked Med-El devices. Speech recognition is not improved for CI listeners when head movement is permitted (Gifford *et al.*, 2018), however head *orientation* does improve speech recognition in NH and CI listeners (Grange and Culling, 2016b; a), suggesting that specific orientations are more important than movement, and that natural head movements do not result in optimum listening orientations. Furthermore, evidence from hearing-aid research suggests that head movements, when combined with a slow-acting AGC, may distort the spatial representation of sounds. Brimijoin *et al.* (2017) mounted hearing aids on a KEMAR manikin that was attached to a rotating chair. The chair was manually rotated from -90° to +90° with a velocity profile similar to that of a natural head turn. Sound was presented at different angles and levels relative to the manikin, and the motion and audio output of the hearing aids was measured. The results showed that for sources at ±90°, hearing-aid output

ILDs were reduced by approximately 1 dB by the AGC, and the interaction between head movement and the hearing-aid processing (e.g. microphone position and dynamic-range compression) caused the direction of the ILD change to reverse by 1-2 dB at the end of the recorded motion. Increasing the level of the sound during the rotation increased this reversal effect, resulting in a change in ILD of up to 3 dB. The authors argued that these changes were perceptually relevant. As noted above, the slow time course and high compression ratios of the AGCs implemented in most contemporary CIs suggest that these perceptual distortions may be even more marked for CI users.

The present study investigates the effect of head movement on the output of bilateral, unlinked Advanced Bionics (AB) CI processors through simulations of both the head movement and the CI processor. The paper is organised into several parts. The first part describes the method used to create the moving source input signal and outlines the parameters of the CI simulation. Subsequent sections present the unilateral CI processor outputs and resulting broadband and narrowband output ILDs that arise from a number of simulated rotational head movements, and discuss the relationship between head movement and AGC. Finally we consider limitations and implications of our simulations, together with the extent to which our results can be generalised to AGCs implemented by the different CI manufacturers.

II Methods

A Overview

We first measured the attack and release times of the AB AGC using the standardized ANSI method (ANSI, 2003), whereby a 35 dB increase and decrease in level are imposed on a 2-kHz sinusoid. We then simulated the effect of this AGC using speech-shaped noise (SSN), which was created from the average spectrum of a subset of the IEEE corpus (Stacey and Summerfield, 2007). Head movement was simulated by convolving segments of the SSN input signal with a 5° resolution hearing-aid microphone impulse response library (Kayser *et al.*, 2009). By interpolating between recorded impulse responses, the perception of a static source changing position relative to a moving head was created. Figure 1a shows a schematic of the method used. This method has been perceptually validated by Brimijoin *et al.* (2013). The moving SSN signal was then input into the MATLAB CI simulation supplied with the “Advanced Bionics Bionic Ear Programming System Plus (BEPS+)” research software platform (Advanced Bionics, 2014). Figure 1b shows a schematic of the system. The resulting output was obtained from the tone vocoder output of the simulation, representing the processed signal just before mapping to the electrical dynamic range took place.

B Advanced Bionics dynamic-range compressor

A modified version of the test signal recommended in the ANSI S3.22 (2003) was used. A 2 kHz sinusoid was used that began at an RMS level of -38 dBFS for 5 seconds (dBFS was defined as decibels relative to the full scale or maximum peak level - 0 dBFS - of a digital system), before increasing abruptly to -3 dBFS for 5 seconds, then abruptly decreasing to -38 dBFS for 5 seconds. The test signal was created using the “Oscillator and Signal

Europe PMC Funders Author Manuscripts

Generator" function available from the MathWorks File Exchange (Brimijoin (2012)). A value of -38 dBFS corresponded to an input level of 49 dB SPL, and -3 dBFS to 84 dB SPL. This was similar to the ANSI test signal but had a slightly lower level in order to avoid clipping. The attack time was defined as the time from the abrupt increase in level of the input signal, to the time at which the output level was within 3 dB of the steady-value output for a 90 dB SPL (or in this case 84 dB SPL) input. The release time was defined as the time from the abrupt decrease in the level of the input signal, to the time where the signal was within 4 dB of the steady value output for the 55-(49)-dB-SPL input. Using these definitions and the modified input signal levels, the attack time for the AB compressor was measured using the simulator as approximately 300 ms and a release time of approximately 1900 ms. The effects of these long response times were combined with those of the fast-acting (approx. 3/80 ms attack/release times) compressor (a "dual-loop compressor"), which was applied to signals that increased near-instantaneously in level by more than 8 dB above the control signal produced by the slow-acting compressor. The minimum threshold for the fast-acting compressor was 65 dB SPL. This protected listeners from sudden, loud, transient sounds. The so-called compressive "pumping" of the level during short silences in the target signal, that can result from fast-acting compressors (Boyle *et al.*, 2009), was prevented by the use of a hold timer.

C Input signal

Speech-shaped noise (SSN) was used as the input signal for the simulations. The frequency spectrum of the noise was created using the average spectrum of 30 IEEE sentences (Stacey and Summerfield, 2007) from eight speakers (four male) of British English. A total of 320 sentences were recorded, leading to a total audio duration of 9 minutes 35 seconds. A new segment of SSN was generated for each head movement shown, by applying random phases to the magnitude of each frequency component in spectrum of the concatenated speech, then applying an inverse Fourier transform to produce SSN. This technique was similar to that found in the "Oscillator and Signal Generator" available on the MathWorks file exchange (Brimijoin, 2012). The segments varied in length due to the different durations of head movement used, but all included 10 seconds before the head movement at the starting position of the head, allowing the compressor to stabilize, and at least 2 seconds after head movement at the final position of the head, to capture any changes in level after the head had stopped moving. The input level was set at 60 dB SPL at the left ear, equivalent to -27 dBFS. In order to investigate the effect of only level changes, linear 6 dB ramps of 1, 2 and 4 seconds duration were applied to the SSN noise, starting after 10 seconds at the initial level of the ramp. Initial levels were 54, 57, and 60 dB SPL (+6 dB change), and 60, 63, and 66 dB SPL (-6 dB change). These levels were chosen to investigate the effect of crossing the compressor threshold (approximately 57 dB SPL depending on spectral content) or remaining above threshold at all times during presentation.

D Modeling head movement

An impulse-response library of behind-the-ear hearing aid front microphone (of the three microphones in the hearing aid's linear array) responses was used as a substitution for a CI microphone (Kayser *et al.*, 2009). The library had a spatial resolution of 5°, and the recordings were made in an anechoic chamber with a source-head distance of 3 meters,

using a KEMAR head-and-torso simulator and Siemens Acuris hearing aids. In order to produce a spatialized and smoothly changing source position, an offline “overlap-add” method was used that was similar to the real-time headphone-presentation method described in Brimijoin *et al.* (2013). Head movement was modeled as a linear interpolation over time between two pre-defined angles relative to the source. The angular head movement was constant and not exactly as it would be on a real user’s head. This choice is discussed in Section IV.B. The two closest impulse responses to the current head angle were chosen and linearly interpolated. Interpolation was required given the 5° spatial resolution of the impulse-response library used. The sample rate was 48 kHz. It was split into 2048 sample frames with a 224-sample step size between each frame. Each frame was convolved with the interpolated binaural impulse response to produce a 2-channel signal of 2048 samples duration, of which only the last 256-sample segment was added to the previously concatenated segments, with a 32-sample linear crossfade between the previously concatenated segments and the new segment. The linear crossfade reduced the chance of discontinuities between segments producing transients in the resulting input signal. This method was originally developed to allow moving signals to be produced using reverberant impulse responses without introducing audible discontinuity artefacts. It is used here to produce an approximate simulation of a sound source rotating around a listener’s head.

E CI simulator

The AB BEPS+ CI simulator used a frequency and amplitude modulated tone vocoder. We reproduced an audio signal from the point in the signal chain of the simulator just before the signal was mapped to a pulse train and to the electrical dynamic range. One sinusoid was produced for each active channel, at the centre frequency (CF) of the input analysis filter used. The sinusoids were amplitude modulated using the envelope that the CI processor extracted from each channel. The CI program was produced in BEPS+ (using a map uploaded from a Harmony processor running HiRes and programmed in Soundwave; Advanced Bionics, 2015). All maximum current levels (MCLs) and threshold current levels (TCLs) were set to 200 current units (CU, defined linearly in AB devices) and 20 CU (10% of MCL) respectively. 16 channels were active in the program. Simple sequential stimulation was used, and the filterbank used was “extended low,” producing a frequency bank with a range of 238 to 8054 Hz. The channel cutoff frequencies are shown in Table I. The input signal was downsampled to the processor sample rate of 17.4 kHz. The filters used in the Advanced Bionics research Harmony and clinical Naida processors are implemented in the frequency domain using Fourier-transformed 256-sample windows with a 20-sample overlap. Input dynamic range (IDR) was 60 dB. Hilbert transforms were used to extract the envelope information. Cathodic-anodic (CA) stimulation was used in monopolar mode, with no current steering.

F Output treatment

The output of the vocoder combined all 16 sinusoids in the broadband case and subsets of sinusoids in the narrowband analyses. The output was further smoothed using the “envelope” function in MATLAB, using the “rms” parameter and a 50 ms window. This was done to make the change in level easier to observe after plotting.

G Narrowband 'input' plots

In order to obtain the 'input' ILDs separated into the same frequency bands as the compressed output ILDs, the output of the CI simulator with an input signal at 45 dB SPL (-42 dB FS, left ear) was used, and the pre-emphasis filter was bypassed. This ensured that exactly the same filters were used, and that any differences were due to the pre-emphasis filter and AGC, as the input remained below the compressor threshold at all times

III Results

A Simple level changes

In order to determine the effects of AGC on a simple change in level, non-spatialized SSN signals that changed linearly by ±6 dB in level at rates of ±1.5, ±3, or ±6 dBs^{-1} at 6 different starting levels were input to the simulator.

Figure 2a shows the results of the +6 dB changes. At the slowest increase rate (1.5 dBs^{-1}, left column) and lowest starting level (54 dB SPL, top row), the input and output level changes are identical until the input crosses the AGC threshold at approximately 57 dB SPL, halfway through the movement. The output stays at threshold for the remainder of the change. At the 57- and 60-dB SPL starting levels, the output level does not change from the threshold level. At an increase rate of 3 dBs^{-1} and 54 dB SPL starting level, the output profile is similar to 1.5 dBs^{-1}. At the higher presentation levels, the output level increases from threshold by < 1 dB during the input increase in level. After the increase stops, the output level takes 1 s to return to threshold. At an increase rate of 6 dBs^{-1} at starting level 54 dB SPL, the output level is similar to the input level for most of the duration of the change in level, before decreasing 1-1.5 dB in level over 1 second, back to threshold. The output profiles at 57 and 60 dB SPL starting level are similar, starting at threshold, increasing by 1 dB in the first 0.5 s of the level increase, remaining at this level for 0.5s, and decreasing over 1 second back to threshold after the level change stops.

Figure 2b shows the results from the -6 dB changes. The effect of the AGC is to prevent the output level form changing except when the input level is below the AGC threshold, or when the rate of change is too fast for the compressor to follow, namely at -6dBs^{-1} (right column). At 60 dB SPL starting level, the output profile is the opposite of the level increase conditions at 54 dB SPL, showing no change in the first half of the decrease, then identical to the input level below threshold. At higher starting levels with a -6 dBs^{-1} level change, the output level decreases from threshold by 1-2 dB during the input level change, and increases back to threshold over 0.5 s after the input decrease stops.

These results show that for a signal with a spectrum similar to that of speech, the AGC threshold is around 57 dB SPL. Therefore the level of most sound sources in the environment, including normal speech, would be affected by the AGC.

B Broadband analysis

The simulated sound source in the following simulations is at 0° at a distance of 3 metres in an anechoic room. The results shown are the combined output of all 16 channels, with the

low cutoff frequency of the lowest channel at 0.238 kHz (CF = 0.324 kHz), and the high cutoff frequency of the highest channel at 8.054 kHz (CF = 5.895 kHz). Full details of the channel cutoff frequencies are shown in table I.

1 Head movement from -30° to +30°—Figure 3 shows the head movement (row one), left and right input/output levels (rows two and three respectively), and input/output ILDs (row four) for a 60° head movement from -30° to 30° over 2 seconds (left column), 1 second (middle column) and 0.5 seconds (right column). These changes correspond to rotational velocities of $30°s^{-1}$, $60°s^{-1}$, and $120°s^{-1}$ respectively. With the head at -30° relative to the source at 0°, the input level at the left ear is set at 60 dB SPL, and the level at the right ear is approximately 5 dB higher. Movement of the head results in a smooth increase in input level (grey lines) at the left ear and decrease in level at the right, until the head stops moving at 30°, the levels stop changing, and the levels at each ear are reversed compared to their starting levels, leading to a reversal of the sign of the ILD (bottom row). These level changes are the same across the three rotational velocities simulated. The changes in output levels (black lines) during head movement are not so homogeneous. The output levels at each ear are approximately the same when the head is not moving, producing an ILD of <1 dB. This is due to the high (12:1) compression ratio used and because both the left and right signals are above the compressor threshold of approximately 57 dB SPL. When the head starts moving at a rotational velocity of $30°s^{-1}$ (left column), the level at the left ear increases and the level at the right ear decreases by approximately equal amounts, resulting in a maximum absolute ILD of 2 dB. This minimum is reached after 1 second of movement and remains constant for the remainder of the head movement, before increasing back to 0 dB 0.5 seconds after the head has stopped moving. At $60°s^{-1}$ (middle column), the maximum absolute ILD induced by the head movement is twice that induced by the $30°s^{-1}$ movement (4 dB). This occurs at the end of the movement, and immediately begins to increase after the movement stops, taking 1 second to return to 0 dB. At $120°s^{-1}$, the ILD profile is similar to the $60°s^{-1}$ plot, however the maximum absolute ILD at the end of the movement is 6 dB, 1 dB less than the natural ILD, and the ILD takes over 1 second to return to 0 dB. Hence the AGC produces marked distortions in the way ILD changes over time – for example being smaller than the input change at the start of the head movement, and producing substantial output changes after the head movement has stopped. Broadband ILD magnitudes > 1 dB appear only when head movement occurs, meaning this is the only situation in which the listener has access to usable broadband ILDs. During head movement, the direction of change in the input and output ILDs are correlated, and this correlation increases with increasing rotational velocity. However, the output ILD is initially of the opposite sign to the input ILD.

2 Head movement from -60° to +60°—Figure 4 shows the head movement (row one), left and right input/output levels (rows two and three respectively), and input/output ILDs (row four) for a 120° head movement from - 60° to 60° over 4 seconds (left column), 2 seconds (middle column) and 1 second (right column). These changes correspond to rotational velocities of $30°s^{-1}$, $60°s^{-1}$, and $120°s^{-1}$ respectively. With the head at -60° relative to the source at 0°, the input level at the right ear is approximately 6 dB higher than the left. Movement of the head results in similar results to those seen in the ±30° case. As in the ±30°

case, the changes in output levels during the head movement are partially dependent on the rotational velocity of the movement. The output levels at each ear are approximately the same when the head is not moving, producing an ILD of <1 dB. When the head starts moving at a rotational velocity of $30°s^{-1}$, the level at the left ear increases and the level at the right ear decreases by approximately equal amounts, resulting in a maximum absolute ILD of 2.5 dB. This minimum is reached after 2 seconds of movement and remains constant for 1 second, then increases back to 0 dB by the time the head has stopped moving. At $60°s^{-1}$, the maximum absolute ILD induced by the head movement is 4.5 dB. This occurs after 1.5 seconds of movement, and immediately begins to increase after this, taking 1 second to return to 0 dB, 0.5 seconds after the head has stopped moving. At $120°s^{-1}$, the ILD profile is again similar to the $60°s^{-1}$ plot, however the maximum absolute ILD of 7 dB, equal to the maximum natural ILD magnitude, is reached 0.2 seconds before the end of the movement. The ILD again takes 1 second to return to 0 dB, 0.8 seconds after the head movement has stopped. As in the ±30° case, the AGC again produces marked distortions in the way ILD changes over time, similar to those produced for the 60° movement (Figure 3).

3 Head movement from -60° to +60° and back—Figure 5 shows the head movement (row one), left and right input/output levels (rows two and three respectively), and input/output ILDs (row four) for a head movement from -60° to 60° to -60° over 8 seconds (left column), 4 seconds (middle column) and 2 seconds (right column). These changes correspond to rotational velocities of $30°s^{-1}$, $60°s^{-1}$, and $120°s^{-1}$ respectively. During the head movements, the input levels show an increase and decrease with a range of 6 dB at the left ear, and an equal and opposite change at the right ear, resulting in an ILD change from 6 to -6 and back to 6 dB. At $30°s^{-1}$, the AGC interacts with the level change induced by the head movement to produce changes in output ILD that are much smaller than at the input, as in the previous cases. The minimum and maximum (±2 dB) of the output ILDs occur when the input ILD is approximately 0 dB, and the output ILDs are 0 dB at the beginning, middle and end of the head movement, when the input ILD is at its maximum or minimum.

At $60°s^{-1}$ the output level changes between the left and right ears are not symmetric as the head turns clockwise and then counterclockwise, resulting in the minimum and maximum output ILDs (±4.5 dB) occurring earlier in time than the minimum and maximum input ILDs, and continuing to change for 0.5 seconds after the head has stopped moving. This is because output levels at each ear halfway through the movement (where previous movements stopped) are different from their starting values. Therefore, when the head moves in the opposite direction in the second half of the movement, the gain reduction applied by the slow-acting AGC is different, and the ILDs produced are not symmetric. At $120°s^{-1}$, the output level of the left ear is more asymmetric than during slower movements, resulting in a minimum level at the end of the head movement that produces a very large positive ILD (11.5 dB), 5 dB larger than the input ILD at the same point, and 4.5 dB larger than the absolute value of the minimum output ILD. After the head stops moving, ILD takes 1.3 seconds to decrease to 0 dB. As in the previous examples, the AGC distorts the ILD cues. At slower velocities, the maximum output ILD magnitudes are smaller and out of phase with the input ILDs. As the head moves faster in a continuous counter clockwise and

clockwise motion, the distorted ILD cues are more in phase with the input ILDs. Their maximum extent may also surpass the natural ILD with a sufficiently rapid rotation.

C Narrowband analysis

As stated in the Methods section, in addition to calculating the input ILDs directly as in the broadband case (figures 3-5), the narrowband ILDs (in each frequency channel) were also calculated. Here we describe the results of those single-channel analyses, using signals above (60 dB SPL equivalent) and below (45 dB SPL equivalent) the AGC threshold. Simulations of levels below the AGC threshold provide a reference that describes the ILDs without any effect of the AGC. As before, the RMS level was set using the level at the left ear.

Figure 6 shows the above and below AGC threshold ILDs for a source at 0° and head movement from -60° to 60° at $60°s^{-1}$, identical to the simulated movement in the middle column of Figure 4. The channels increase in frequency left to right and top to bottom across the six subplots. Before head movement, when the head is static, the sub-threshold ILDs generally increase with frequency from 2 to 17 dB. Supra-threshold ILDs also increase with frequency, however all the ILDs are reduced, producing negative ILDs at low frequency (-7 dB in the channel with f_c = 0.324 kHz) and maximum high-frequency ILDs of 6 dB (channel with f_c = 2.845 kHz). The negative ILDs occur for two reasons. The pre-emphasis (high-pass) filter is applied before compression, meaning the compressor is driven by the high-frequency components of the input signal. ILDs are larger at high frequencies. The AGC is also broadband, so the same level reduction is applied across all frequencies. A greater level reduction is applied to the higher level, ipsilateral ear, resulting in the ILD inversion at low frequencies. The individual channel plots also reveal differences in the ILD profiles from channel to channel. ILDs increase by 1-2 dB as the head starts moving towards the source in in the channels with f_c = 1.759 and 5.896 kHz.

IV Discussion

A Simple, broadband and narrowband analysis

For the level changes simulated here, slow (1.5 and 3 dBs^{-1}) changes in input of ±6 dB above the compression threshold produce little or no change in output level. This is predicted and explained by the high compression ratio (12:1) used, which means that an increase in output level of 1 dB above threshold would require the input to be 12 dB above threshold. When presented with a rapid input level increase (6 dBs^{-1}), the output level first increases above threshold, then returns to threshold. This is due to the slow attack time (300 ms) used by the AGC.

The output of a CI processor on a rotating head when presented with continuous speech-shaped noise was simulated. In particular, the interaction between the independent, unlinked AGC and level changes at each ear due to head movement was investigated. The simulated moving input signals showed the expected change in level and corresponding change in broadband ILDs, in agreement with previous similar studies (Brimijoin *et al.*, 2017). The AGC had a large effect on the output levels at each ear, equalizing the output levels.

Europe PMC Funders Author Manuscripts

Broadband and high-frequency absolute ILDs are reduced by AGC when the head is not moving. This reduction in static ILD due to unlinked AGC has been reported previously (Wiggins and Seeber, 2011; Dorman *et al.*, 2014). Input (or sub-threshold) ILDs at low frequencies are close to 0 dB. Applying high-frequency pre-emphasis and broadband AGC to each signal means that the level reduction will be driven by the high frequencies, but applied equally across frequency. In addition, signals at the contralateral ear will be low-pass filtered due to the acoustic head shadow. Therefore, a reduction in high-frequency ILD induces a low-frequency ILD that is equal to that reduction, with the opposite sign. Similar results have also been reported by Dorman *et al.* (2014) for static ILDs. The results presented here are the first to show the changes in ILD that occur due to the interaction between CI AGC and head movement. In a dynamic situation, the attack and release times of the AGC alter the profile of the ILDs based on the speed and duration of movement in a way that was previously only hinted at in similar studies of hearing aids (Brimijoin *et al.*, 2017), which generally have relatively fast acting dynamic-range compressors that are more complex (i.e. multi-channel compressors), weaker (i.e. compression ratios below 2 or 3:1), and faster (i.e. attack and release times of the order of tens of milliseconds).

When combined with head movement at different rotational velocities, the extent and profile of the output ILDs were fundamentally altered compared to the input ILDs. In the broadband case, as rotational velocity increased, the maximum absolute ILD induced by the interaction between the unlinked AGC and movement also increased, and the change in output ILD correlated more with the change in input ILD. The extent of the rotation had a comparatively small effect on maximum absolute ILD. The larger the absolute ILD induced by head movement, the longer it took for the AGC to stabilize the output levels and return the ILD to near 0 dB. This could result in the ILD continuing to change for up to 1.3 seconds after the head had stopped moving. Therefore a faster head movement produces a larger after effect once the head has stopped moving. The size of this after-effect depends on the maximum magnitude of the output ILD, not the input ILD (as shown in Figures 3-5). The narrowband analysis showed that the broadband dynamic ILD profile was caused by highly variable ILD changes in each frequency band. They could be summarised as follows: during a movement from -60° to 60°, the narrowband ILDs initially converge on a single ILD value at some point during the head movement, then diverge again (e.g. the ILD in the channel with f_c = 0.324 kHz changes from -7 dB to 7 dB, and the ILD in the channel with f_c = 2.845 kHz changes from 6 dB to -6 dB).

The perceptual consequences of these distortions are difficult to quantify from simulation alone. Dorman *et al.* (2014) expected poor static localization from bilateral Med-El CI listeners, due ILD distortions by an AGC with a relatively low 3:1 compression ratio (the AB device uses a 12:1 ratio), resulting in less distortion than reported in this study. They reported that 6 out of 16 CI listeners were found to have good localization ability. This suggests that localisation by those listeners was not substantially degraded by the opposite sign of ILDs at low and high frequencies, and that listeners were perhaps neglecting the low-frequency ILDs when listening to broadband stimuli.

Figure 7 illustrates how a bilateral AB CI listener may perceive sound sources through unlinked bilateral AGCs while the head is static and moving. Row 1 shows the possible

perceived position if the perceived location is based on the broadband ILDs (grey circles). At the beginning of the movement (column A), the broadband output ILD is 0 dB, which would put the location of the sound directly in front of the listener, at -60° relative to the actual source position (black circles). After 1 second (B), the head has moved 60° clockwise and the source is directly in front of the listener. The broadband output ILD is -3 dB, and could be perceived at -30° relative to the listener. In column C, at the end of the movement, the output broadband ILD is still negative and decreasing, which could be perceived as the source moving towards the front of the listener. 0.5 seconds after the head has stopped moving, the output broadband ILD has stabilized at 0 dB, placing the source at 60° from the actual source position, directly in front of the listener. Row 2 shows the more complicated case of the combined narrowband ILDs (grey ovals, dark grey for low frequencies, and light grey for high frequencies). The exact perceived position will depend on the perceptual weights given to each frequency band. However what is clear is that as the narrowband ILDs are initially both positive and negative (A), the source may have a wide angular extent when the head is static. This has been reported previously (Wiggins and Seeber, 2011). During movement (B), the width of the sound may be reduced, as the ILDs converge on a single value. By the end of the movement (C), the high and low frequency ILDs swap position compared to the start position, and diverge (D). Row 3 shows the possible position of the sound source if the listener used only a single, high-frequency (channel with f_c = 2.845 kHz) ILD. In this case, the reduced ILD may move the perceived position closer to the front of the listener (A). During movement, the source may be perceived as straight ahead (0 dB ILD) when its physical position relative to the head is still several degrees clockwise of the listener (B). At the end of the movement, the source may be perceived to be anticlockwise of the listener. No further change in ILD occurs in this channel (D). The extent to which listeners overcome these distortions will depend on how they weight high- and low-frequency ILD cues both when the source and head are static and when the head is moving.

It is important to highlight that though the output ILDs during head movement are very different to the input ILDs, one is positively correlated with the other, and this correlation increases as the rotational velocity increases. The change in output ILDs are systematic, but affected more by rotational velocity than the position of the source. Therefore they could be used to disambiguate front-back confusions, but perhaps not allow the position of a source to be determined.

Studies using static heads and sources have shown that the distortion of ILDs by unlinked AGC is particularly important for bilateral CI users, as they rely more on ILDs than ITDs for localization of sources (Bronkhorst, 2000; van Hoesel et al., 2002; van Hoesel and Tyler, 2003; Seeber and Fastl, 2008; van Hoesel et al., 2008). Arguably, the production of ILDs during head movements that bore little or no resemblance to the true ILD could be a more serious problem than the reduction in absolute ILDs due to unlinked AGC in the static case. If ILD was always at or close to 0 dB, regardless of where a source was relative to the listener, then listeners could be expected to stop relying on this cue. However, if head (or indeed, source) movement were to induce non-zero dynamic ILDs with little relation to the true ILD, listeners may try to use them to localize a source, which would result in - at best - slower localization, and at worst a complete failure to localize the source. The conflicting cues provided by different frequency channels are likely to at least add another level of

complexity to the listener's attempts to localize. Previous work investigating the effect of unlinked compression on ILDs has suggested that linking AGCs and applying the gain reduction in the processor on the ipsilateral ear to the processor on the contralateral ear would preserve static ILDs (Wiggins and Seeber, 2013). This would be likely to preserve ILDs during head movements. However, the limited electrical dynamic range of many CI listeners may mean that reducing the level of sound further in one ear reduces any advantage in speech intelligibility that the listener has gained from bilateral listening. In addition, linked compressors may introduce unnatural level changes at each ear that could have detrimental effects on localization ability and speech intelligibility.

The ILD distortions shown in this study for a static source and a moving head would also occur in the opposite case, where the head was static and the source was moving. However, sound sources rarely move in a perfect circle around the head. It is common for a moving sound source to move in a straight line across the listener (e.g. traffic when waiting to cross a road). Even the fastest head movements described here, as shown in the right column of figure 4 (±60°, 120°s^{-1}), would equate to a straight-line speed of 37.4 kmh^{-1} (assuming a source-listener distance of 3 metres at 0°), which is comparable to slow-moving vehicular traffic. Motion in a straight line across the listener's front hemifield would cause an increase and decrease in level of ±3 dB, which may also induce further level and ILD distortions. The sound of traffic moving from right to left (equivalent to the head movement used here) and then stopping may appear initially to move left, then move backwards to the acoustic midline.

The effect of a diffuse background noise or reverberation on these results should also be considered. This would add equal amounts of energy to the signal reaching each ear. This would increase the level of the contralateral ear more than the ipsilateral, as adding the same amount of energy to the lower level ear would have a relatively larger effect when measured on a decibel scale. This would reduce the natural input ILD across frequencies for a given source angle (Ihlefeld and Shinn-Cunningham, 2011). The overall effect would be to reduce the ILD magnitudes during head movements, resulting in the output ILD in diffuse noise during the 120° head movement appearing more similar to the output ILD for the 60° head movement. The distribution of so-called "instantaneous ILDs" (Catic *et al.*, 2013) is also increased when a diffuse noise is present, though this distribution would not be affected by the slow AGC used here.

The combined results of these simulations suggests that the AGC employed in contemporary CIs may make a listener's auditory environment more dynamic than it really is: static sources may appear to move during head movements and *continue* to move after the head has stopped moving. It may make the auditory environment narrower in angular extent: output ILDs are rarely as large as the input ILDs, except under the most extreme head movements simulated. And it may change the perceptual "width" of sounds: the range of ILDs as a function of frequency changes in an unnatural way during head movements.

B Future work and limitations

What is clear from the presented simulations is that the output ILDs are highly distorted and may be more difficult for the listener to use reliably. Overall, average broadband ILDs are <1

dB when the average level of the source is above the AGC threshold and the head is static. When the head moves, an output ILD will be induced that depends more on the head's rotational velocity than on the position of the source, and the sign of the output ILD will initially be opposite to the input ILD. Eventually, during longer head rotations, the AGC acts to return the levels at the two ears to threshold. If the head turn is short, the AGC equalizes the levels between the ears after head rotation has stopped. Since the change in ILDs would initially be in the same direction as the input ILDs (although of opposite sign), listeners may be able to learn to use these distorted cues in a useful way, such as for front-back disambiguation.

The simulation presented here could be improved in a number of ways in the future. Currently, the simulation uses perceptually validated approximations of the microphone signals that would be recorded on a moving head (Brimijoin *et al.*, 2013). Real head movements are generally more sinusoidal than the linear head movements used in this study, with periods of acceleration and deceleration at the beginning and end of the movements. To produce the same average velocity, the sinusoidal movement would include a central portion that was faster than the equivalent linear movement. Therefore, dependent on the duration of the acceleration and deceleration periods of the movement, the changes in ILD for a 30°/s sinusoidal movement may look more like a linear 60°/s movement. Future work will use signals recorded from moving manikin heads and human CI listeners, producing more realistic movements to be compared to the simple linear movements used here.

The present simulations cover only the processing used in AB devices. The different AGC settings used in other manufacturers' devices could have large effects on the changes in output level due to head movement (Vaerenberg *et al.*, 2014). The Med-El device uses a broadly similar system to the one described here (Stöbich *et al.*, 1999), but with a much lower compression ratio (Dorman *et al.*, 2014) and faster attack and release times of 100 and 400 ms. The smaller compression ratio means that the output ILDs will be less distorted, both when the head is static and moving. The faster attack and release times in the Med-El system would respond more quickly to changes in level than the Advanced Bionics system, meaning that the ILD profile during head movement may be more similar to the natural ILD profile. In addition, the compression threshold can be adjusted from 48 dB SPL (100% "sensitivity") to 67 dB SPL (0% "sensitivity"). This may partially explain why recent work by Pastore *et al.* (2018) shows that bilateral Med-El users are able to resolve front-back confusions using head movement and changes in ILD. The sensitivity settings of the listeners' devices varied from 50% (52.75 dB SPL) to 75% (57.5 dB SPL) and the high-frequency Gaussian noise stimuli were presented at 60 dBA. ILD measurements by Dorman *et al.* (2014) using similar stimuli, source position and CI settings produced an average ILD across frequency of 6 dB. Changes in an ILD of this magnitude were sufficient for listeners to resolve front-back confusions. The Cochlear Ltd. device uses a slow-acting automatic sensitivity control (ASC), followed by a fast-acting limiter (e.g. a compressor with an infinite compression ratio), and Adaptive Dynamic Range Optimization (ADRO) after the filterbank (James *et al.*, 2002; Khing *et al.*, 2013). It is difficult to predict how these cascaded slow- and fast-acting systems would affect the response to dynamic ILDs. The stimulation strategy used in Cochlear Ltd. devices differs substantially from the continuous interleaved sampling (CIS) strategy used in other manufacturers' processors. The advanced

combination encoder (ACE) strategy selects the 8 most energetic frequency bands out of 22 in each 8 ms time window, and stimulates the corresponding electrodes (Vandali *et al.*, 2000; Laneau, 2005). Kelvasa and Dietz (2015) have found that head-shadowing results in more low-frequency peaks being selected in the contralateral ear relative to the ipsilateral ear, in some cases resulting in an ILD with the opposite sign at low-frequencies compared to high frequencies. They found this to be comparable to the effect of dynamic-range compression found by Dorman *et al.* (2014). Thus, ILDs could be distorted at multiple points along the CI signal path.

The threshold (or "sensitivity") settings of both the Med-El and Cochlear Ltd devices can be adjusted by audiologists, meaning that the amount of compression (and thus ILD distortion) applied to sound sources at normal listening levels could be reduced relative to the AB device. The Oticon device does not use a front-end compressor. Multiband, instantaneous compression is applied at the end of the signal chain, at the same time as the acoustic envelope is mapped to the electrical domain (Bozorg-Grayeli *et al.*, 2016). Instantaneous compression may distort the envelope of modulated sounds such as speech above the compression threshold. Therefore ILD compression may still occur, but the dynamic ILD profiles during head movement may be very different to the results shown in this study.

V Conclusions

A simulation of bilateral CI processors on a rotating head was used to investigate the effect of unlinked AGC on output ILDs during different speeds and extents of head movement. It was found that the interaction between AGC and head movement induces ILDs that were very different from the input ILDs. The output ILD was more strongly affected by the speed and duration of head movement than by the actual position of the source relative to the head. The slow attack/release AGC used in many CI processors resulted in output ILDs that continued to change after head movement had stopped, particularly for fast, short-duration head movements. An analysis of narrowband ILDs showed that the AGC induced non-zero low-frequency ILDs with the opposite sign to the high-frequency ILDs, and head movement caused the distribution of ILD across frequency to change in an unnatural way. The size of the induced output ILDs are large enough to be perceived by CI listeners, and may substantially degrade the perception of sound location.

Acknowledgements

This work was supported by a Pauline Ashley fellowship PA19 from Action on Hearing Loss to A. A-B. and by Award No. RG91365 from the Medical Research Council to R.P.C. The authors wish to thank Patrick Boyle from Advanced Bionics for technical support.

References

Advanced Bionics. Bionic Ear Programming System Plus. Valencia, CA, USA: 2014.

Advanced Bionics. Soundwave 2.3. Valencia, CA, USA: 2015.

Agterberg M. Hearing with acoustic hearing implants, proposal multicenter study towards treatment options for patients with a contra indication for hearing aids. Journal of Hearing Science. 2018; 8

ANSI. ANSI S3.22-2003: Specification of hearing aid characteristics. American National Standards Institute; New York: 2003.

Archer-Boyd AW, Holman JA, Brimijoin WO. The minimum monitoring signal-to-noise ratio for off-axis signals and its implications for directional hearing aids. Hear Res. 2018; 357:64–72. [PubMed: 29223929]

Boyle PJ, Buechner A, Stone MA, Lenarz T, Moore BCJ. Comparison of dual-time-constant and fast-acting automatic gain control (AGC) systems in cochlear implants. Int J Audiol. 2009; 48:211–221. [PubMed: 19363722]

Bozorg-Grayeli A, Guevara N, Bebear J-P, Ardoint M, Saai S, Hoen M, Gnansia D, Romanet P, Lavieille J-P. Clinical evaluation of the xDP output compression strategy for cochlear implants. European archives of oto-rhino-laryngology. 2016; 273(Supplement):2363–2371. [PubMed: 26476927]

Brimijoin, WO. Oscillator and Signal Generator. 2012. The function can be downloaded from the MathWorks File Exchange, https://www.mathworks.com/matlabcentral/fileexchange/37376-oscillator-and-signal-generator

Brimijoin WO, Akeroyd MA. The role of head movements and signal spectrum in an auditory front/back illusion. i-Perception. 2012; 3:179–182. [PubMed: 23145279]

Brimijoin WO, Boyd AW, Akeroyd MA. The contribution of head movement to the externalization and internalization of sounds. PlOS One. 2013; 8

Brimijoin WO, McLaren AI, Naylor GM. Hearing impairment, hearing aids, and cues. Proceedings of Meetings on Acoustics. 2017; 28

Bronkhorst AW. The cocktail party phenomenon: A review of research on speech intelligibility in multiple-talker conditions. Acta Acustica united with Acustica. 2000; 86:117–128.

Catic J, Santurette S, Buchholz JM, Gran F, Dau T. The effect of interaural-level-difference fluctuations on the externalization of sound. J Acoust Soc Am. 2013; 134:1232–1241. [PubMed: 23927121]

Dorman MF, Loiselle L, Stohl J, Yost WA, Spahr AJ, Brown C, Cook S. Interaural level differences and sound source localization for bilateral cochlear implant patients. Ear Hear. 2014; 35:633–640. [PubMed: 25127322]

Ege R, van Opstal AJ, Bremen P, van Wanrooij MM. Testing the Precedence Effect in the Median Plane Reveals Backward Spatial Masking of Sound. Scientific Reports. 2018; 8

Gifford RH, Loiselle L, Natale S, Sheffield SW, Sunderhaus LW, Dietrich MS, Dorman MF. Speech understanding in noise for audlts with cochlear implants: effects of hearing configuration, source location certainty, and head movement. Journal of Speech, Language, and Hearing Research. 2018; 61:1306–1321.

Goman, AM. Psychology. University of York; 2014. A comparison of bilateral cochlear implantation and bimodal aiding in severely-profoundly hearing-impaired adults: head movements, clinical outcomes, and cost-effectiveness.

Grange JA, Culling JF. Head orientation benefit to speech intelligibility in noise for cochlear implant users and in realistic listening situations. J Acoust Soc Am. 2016a; 140:4061–4072. [PubMed: 28039996]

Grange JA, Culling JF. The benefit of head orientation to speech intelligibility in noise. J Acoust Soc Am. 2016b; 139:703–712. [PubMed: 26936554]

Grantham DW, Ashmead DH, Ricketts TA, Haynes DS, Labadie RF. Interaural time and level difference thresholds for acoustically presented signals in post-lingually deafened adults fitted with bilateral cochlear implants using CIS+ processing. Ear Hear. 2008; 29:33–44. [PubMed: 18091105]

Hassager HG, Wiinberg A, Dau T. Effects of hearing-aid dynamic range compression on spatial perception in a reverberant environment. J Acoust Soc Am. 2017; 141:2556–2568. [PubMed: 28464692]

Ihlefeld A, Shinn-Cunningham BG. Effect of source spectrum on sound localization in an everday reverberant room. J Acoust Soc Am. 2011; 130:324–333. [PubMed: 21786902]

James CJ, Blamey PJ, Martin L, Swanson BA, Just Y, Macfarlane D. Adaptive dynamic range optimization for cochlear implants: a preliminary study. Ear Hear. 2002; 23:49S–58S. [PubMed: 11883767]

Kayser H, Ewert SD, Anemueller J, Rohdenburg T, Hohmann V, Kollmeier B. Database of multichannel in-ear and behind-the-ear head-related and binaural room impulse responses. EURASIP Journal on advances in signal processing. 2009

Keidser G, Rohrseitz K, Dillon H, Hamacher V, Carter L, Rass U, Convery E. The effect of multi-channel wide dynamic range compression, noise reduction, and the directional microphone on horizontal localization performance in hearing aid wearers. Int J Audiol. 2006; 45:563–579. [PubMed: 17062498]

Kelvasa D, Dietz M. Auditory model-based sound direction estimation with bilateral cochlear implants. Trends Hear. 2015; 19

Khing PP, Swanson BA, Ambikairajah E. The effect of automatic gain control structure and release time on cochlear implant speech intelligibility. PLoS ONE. 2013; 8:e82263. [PubMed: 24312408]

Laback B, Pok S-M, Baumgartner W-D, Deutsch WA, Schmid K. Sensitivity to interaural level and envelope time differences of two bilateral cochlear implant listeners using clinical sound processors. Ear Hear. 2004; 25:488–500. [PubMed: 15599195]

Laneau, J. When the deaf listen to music–pitch perception with cochlear implants. Katholieke Universiteit Leuven, Faculteit Toegepaste Wetenschappen; Leuven, Belgium: 2005. Ph. D. dissertation

Mueller MF, Meisenbacher K, Lai W-K, Dillier N. Sound localization with bilateral cochlear implants in noise: How much do head movements contribute to localization? Cochlear implants international. 2014; 15:36–42. [PubMed: 23684420]

Musa-Shufani S, Walger M, von Wedel H, Meister H. Influence of dynamic compression on directional hearing in the horizontal plane. Ear Hear. 2006; 27:279–285. [PubMed: 16672796]

Pastore MT, Natale SJ, Yost WA, Dorman MF. Head Movements Allow Listeners Bilaterally Implanted With Cochlear Implants to Resolve Front-Back Confusions. Ear Hear. 2018; 39:1224–1231. [PubMed: 29664750]

Schwartz AH, Shinn-Cunningham BG. Effects of dynamic range compression on spatial selective auditory attention in normal-hearing listeners. J Acoust Soc Am. 2013; 133:2329–2339. [PubMed: 23556599]

Seeber BU, Baumann U, Fastl H. Localization ability with bimodal hearing aids and bilateral cochlear implants. J Acoust Soc Am. 2004; 116:1698–1709. [PubMed: 15478437]

Seeber BU, Fastl H. Localization cues with bilateral cochlear implants. J Acoust Soc Am. 2008; 123:1030–1042. [PubMed: 18247905]

Skinner MW, LK H, Holden TA, Demorest ME, Fourakis MS. Speech recognition at simulated soft, conversational and raised-to-loud vocal efforts by adults with cochlear implants. J Acoust Soc Am. 1997; 101:3766–3782. [PubMed: 9193063]

Stacey PC, Summerfield AQ. Effectiveness of computer-based auditory training in improving the perception of noise-vocoded speech. J Acoust Soc Am. 2007; 121:2923–2935. [PubMed: 17550190]

Stöbich B, Zierhofer CM, Hochmair ES. Influence of automatic gain control parameter settings on speech understanding of cochlear implant users employing the continuous interleaved sampling strategy. Ear Hear. 1999; 20:104–116. [PubMed: 10229512]

Vaerenberg B, Govaerts PJ, Stainsby T, Nopp P, Gault A, Gnansia D. A uniform graphical representation of intensity coding in current-generation cochlear implant systems. Ear Hear. 2014; 35:533–543. [PubMed: 24681426]

Van Hoesel R. Exploring the benefits of bilateral cochlear implants. Audiol Neurootol. 2004; 9:234–246. [PubMed: 15205551]

van Hoesel R, Böhm M, Pesch J, Vandali A, Battmer RD, Lenarz T. Binaural speech unmasking and localization in noise with bilateral cochlear implants using envelope and fine-timing based strategies. J Acoust Soc Am. 2008; 123:2249–2263. [PubMed: 18397030]

van Hoesel R, Ramsden R, O'Driscoll M. Sound-direction identification, interaural time delay discrimination, and speech intelligibility advantages in noise for a bilateral cochlear implant user. Ear Hear. 2002; 23:137–149. [PubMed: 11951849]

van Hoesel RJM, Tyler RS. Speech perception, localization, and lateralization with bilateral cochlear implants. J Acoust Soc Am. 2003; 113:1617–1630. [PubMed: 12656396]

Vandali AE, Whitford LA, Plant KL, Clark GM. Speech perception as a function of electrical stimulation rate: using the Nucleus 24 cochlear implant system. Ear Hear. 2000; 21:608–624. [PubMed: 11132787]

Veugen LC, Chalupper J, Mens LH, Snik AF, van Opstal AJ. Effect of extreme adaptive frequency compression in bimodal listeners on sound localization and speech perception. Cochlear implants international. 2017; 18:266–277. [PubMed: 28726592]

Wiggins IM, Seeber BU. Dynamic-range compression affects the lateral position of sounds. J Acoust Soc Am. 2011; 130:3939–3953. [PubMed: 22225049]

Wiggins IM, Seeber BU. Linking dynamic-range compression across the ears can improve speech intellibility in spatially separated noise. J Acoust Soc Am. 2013; 133:1004–1016. [PubMed: 23363117]

Zeng F-G, Galvin J. Amplitude compression and phoneme recognition in cochlear implant listeners. Ear Hear. 1999; 20:60–74. [PubMed: 10037066]

Zeng F-G, Grant G, Niparko J, Galvin J, Shannon R, Opie J, Segel P. Speech dynamic range and its effect on cochlear implant performance. J Acoust Soc Am. 2002; 111:377–386. [PubMed: 11831811]

Europe PMC Funders Author Manuscripts

Europe PMC Funders Author Manuscripts

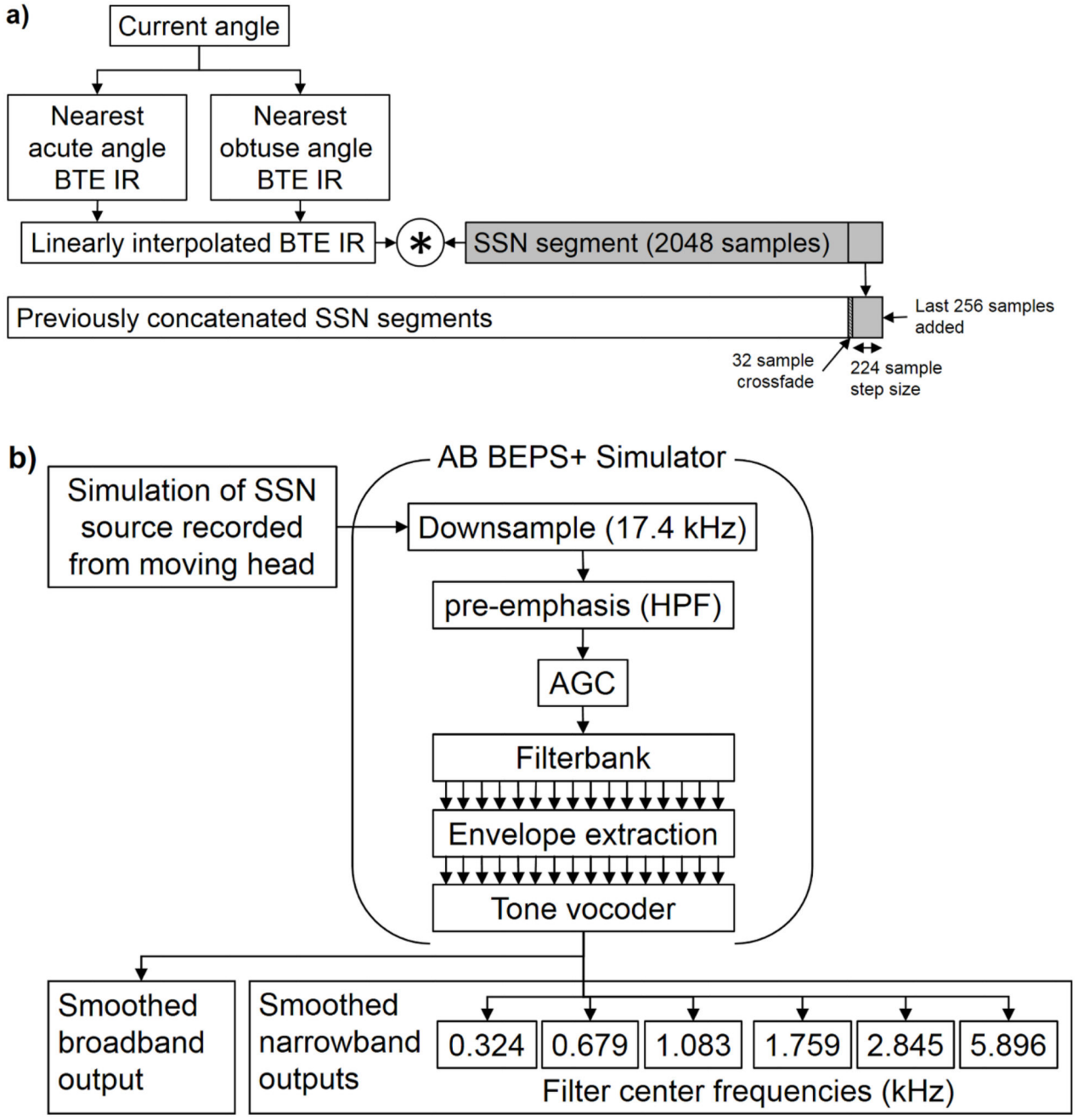

Figure 1.

a) Schematic showing the technique used to simulate a static source incident on a moving head and create a bilateral input signal. b) Schematic showing the signal path for the CI simulator and output.

Europe PMC Funders Author Manuscripts

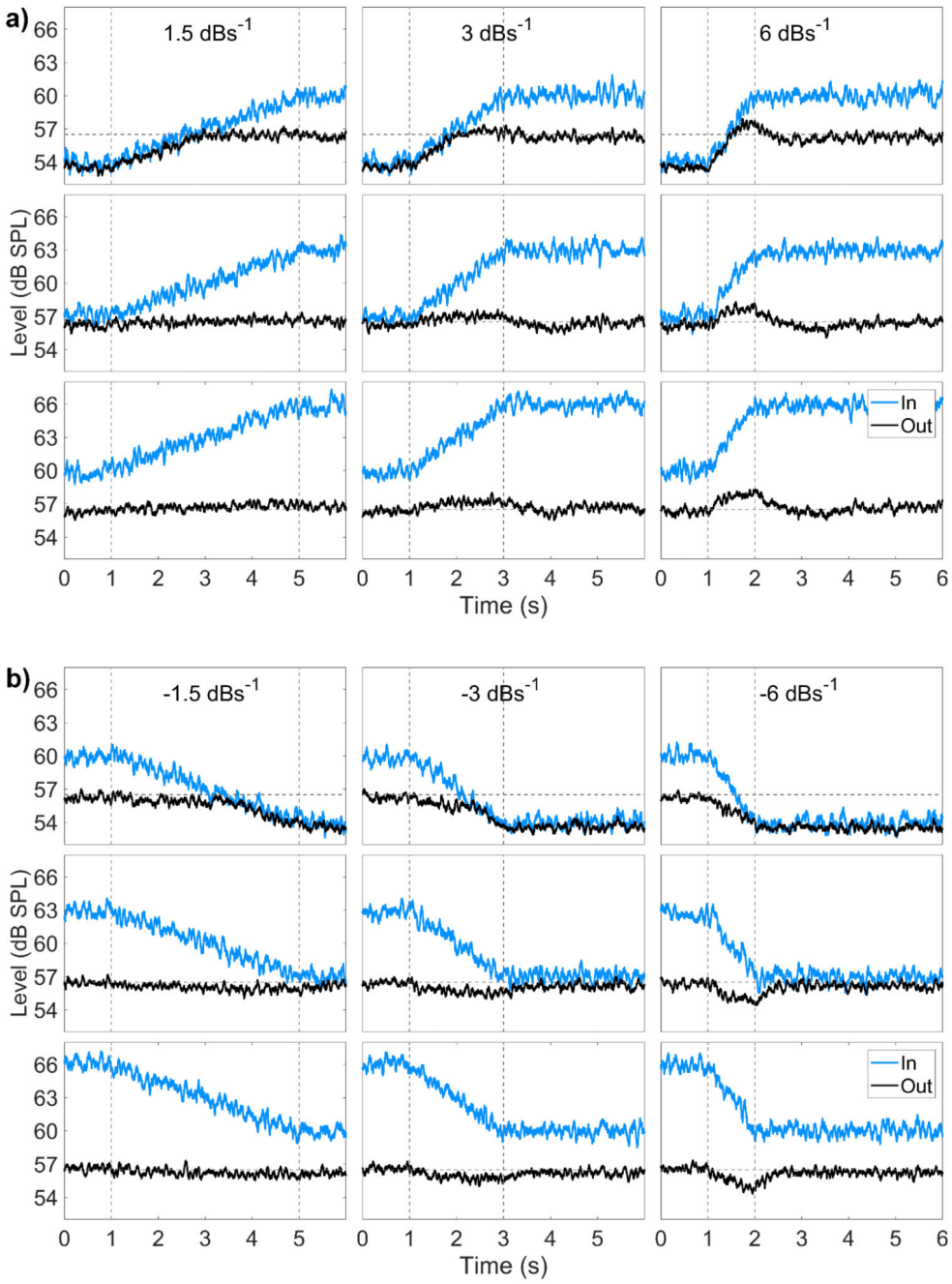

Figure 2.

a) Input and output level changes for +6dB input level increase. Each column displays a different increase rate. Column one (left) shows 1.5 dBs^{-1}, column two (middle) 3 dBs^{-1}, and column three (right) 6 dBs^{-1}. Each row shows a different starting level. Row one shows a starting input level of 54 dB SPL, row 2 57 dB SPL, and row 3 60 dB SPL. Input is shown in grey and output in black. The areas of the plots bounded by the dashed lines show the period of rotational movement. b) The same as 2b, for an input level decrease of -6 dB. Row 1 shows a starting level of 60 dB SPL, row 2 63 dB SPL, and row 3 66 dB SPL.

Europe PMC Funders Author Manuscripts

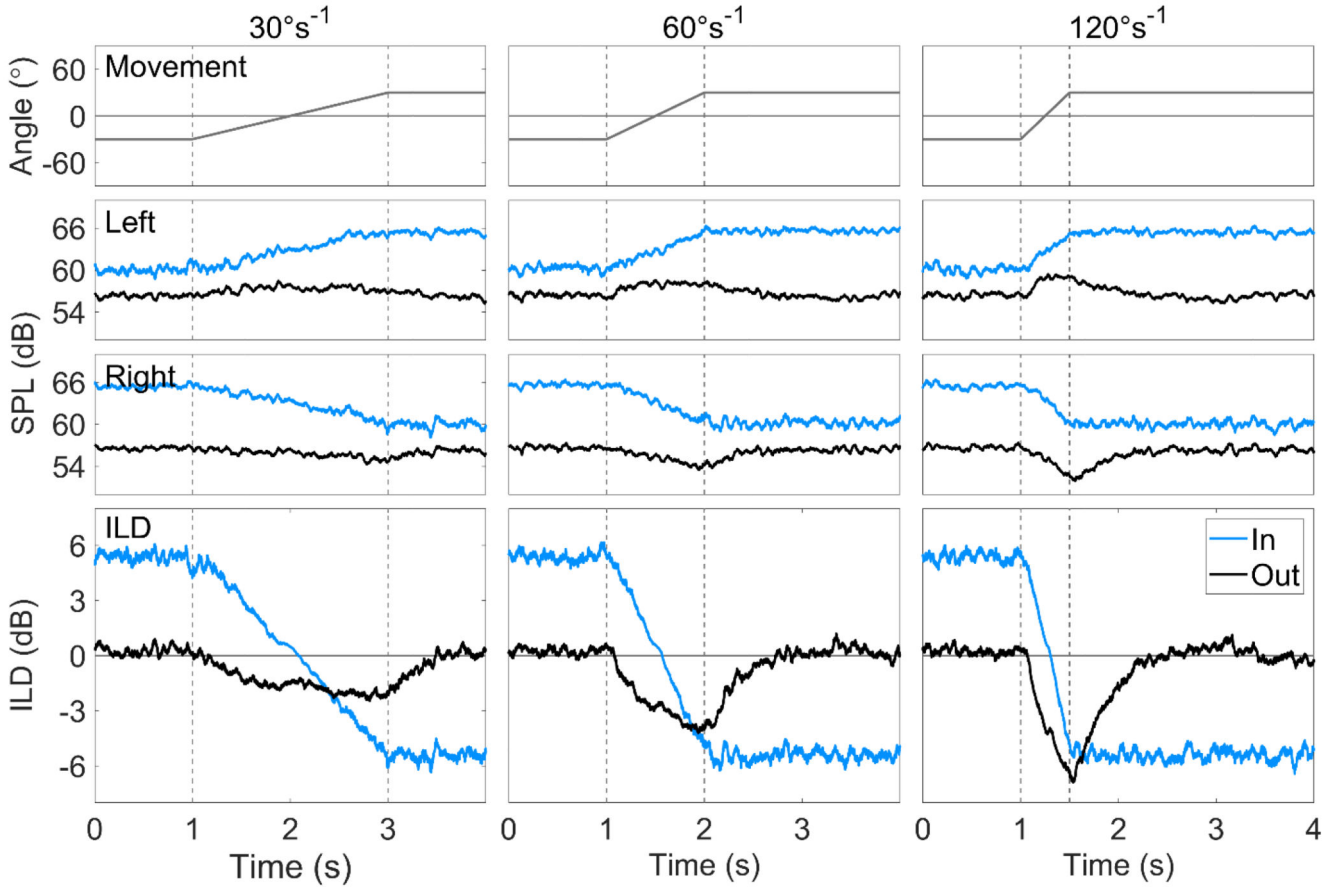

Figure 3.

Head movements, left and right input and output levels, and input and output ILDs plots, for a speech-shaped noise input at 60 dB SPL (left ear). Each column displays a different rotational velocity. Column one (left) shows 30°s^{-1}, column two (middle) 60°s^{-1}, and column three (right) 120°s^{-1}. Row one shows head movement, row two shows the input (grey) and output (black) level of the device at the left ear, row three shows the same for the right ear, and row four shows the input (grey) and output (black) ILDs. The areas of the plots bounded by the dashed lines show the period of rotational movement.

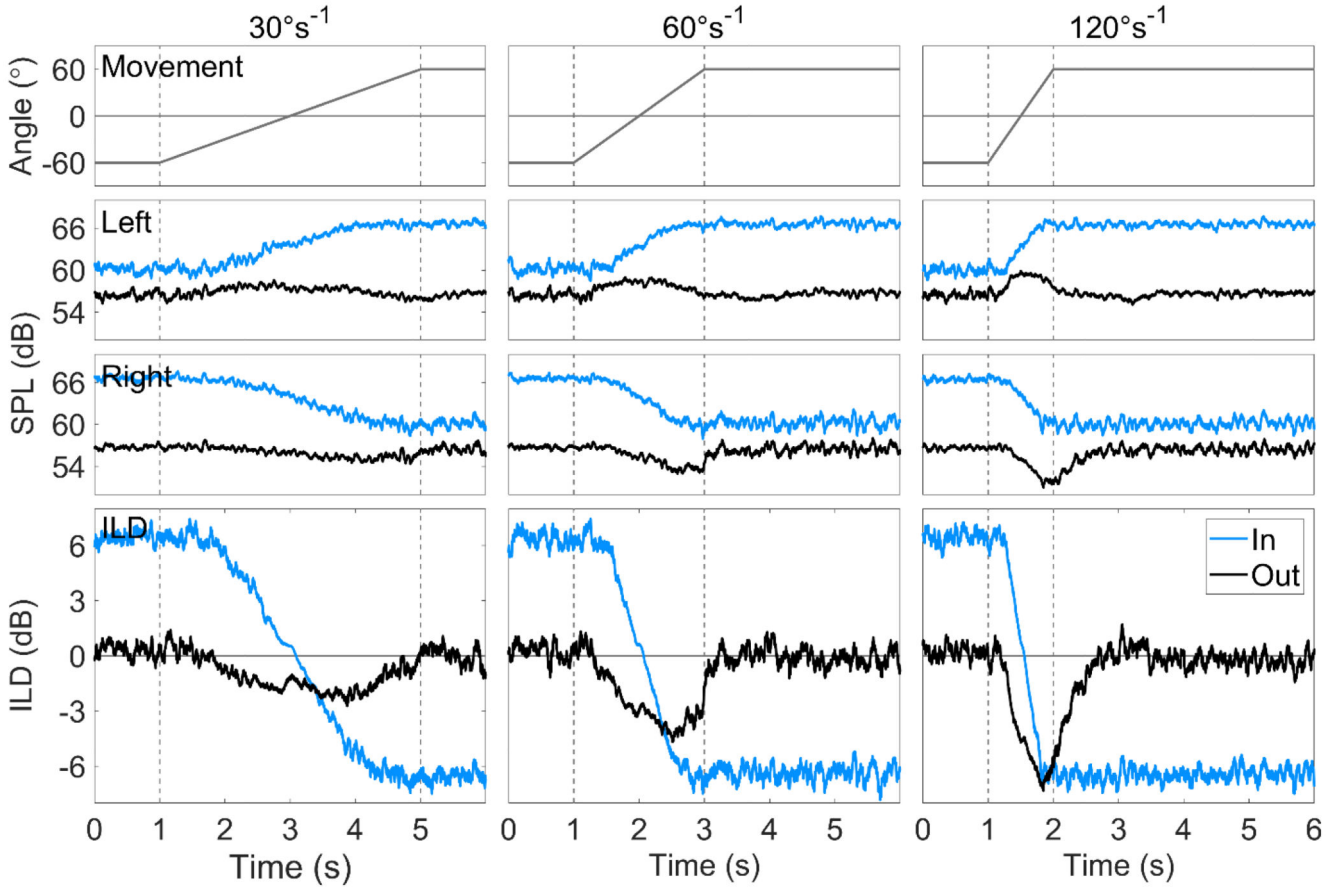

Figure 4.
As figure 3 for head movements from -60° to 60°.

Europe PMC Funders Author Manuscripts

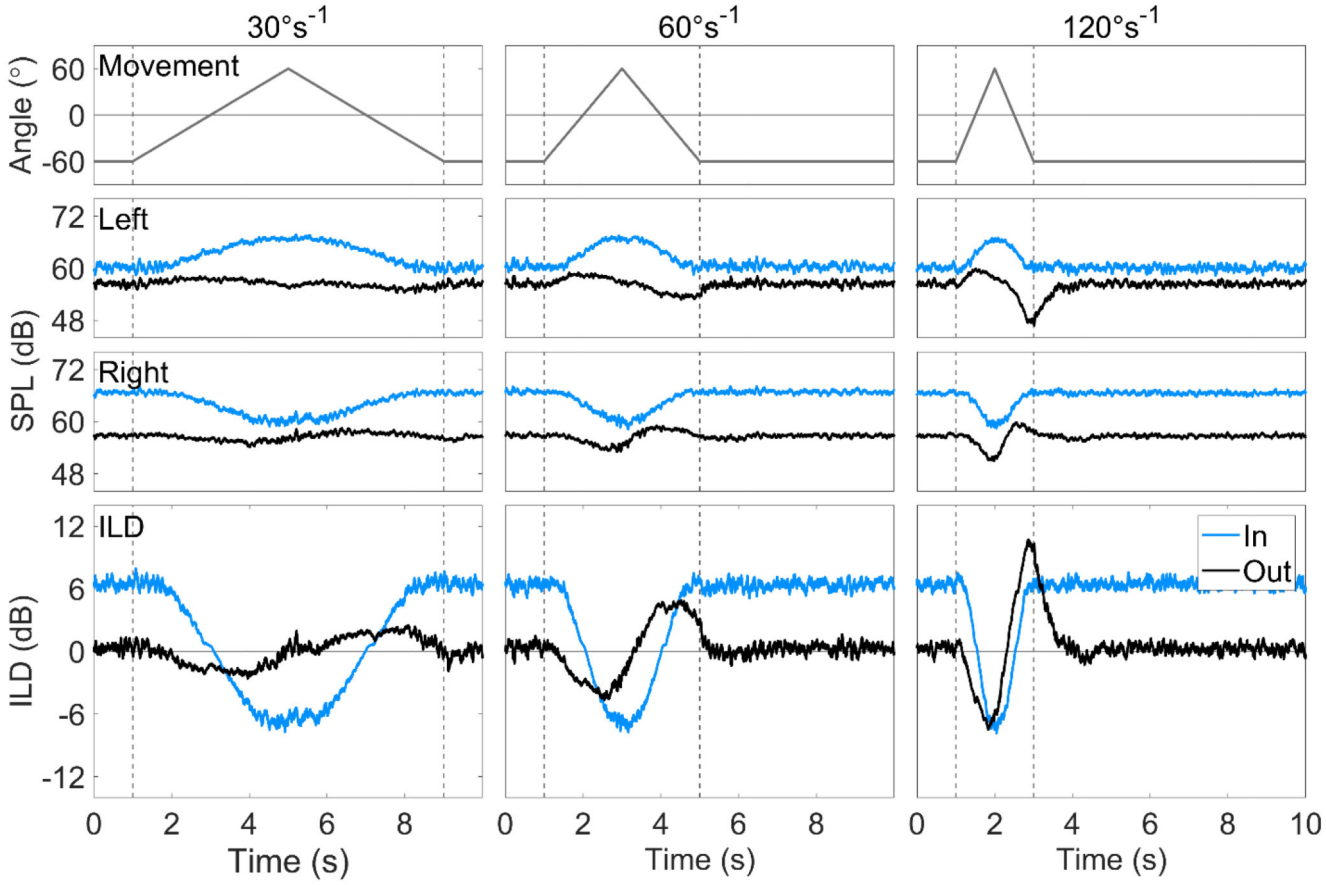

Figure 5.
As figure 3 for head movements from -60° to 60° to -60°.

Europe PMC Funders Author Manuscripts

Europe PMC Funders Author Manuscripts

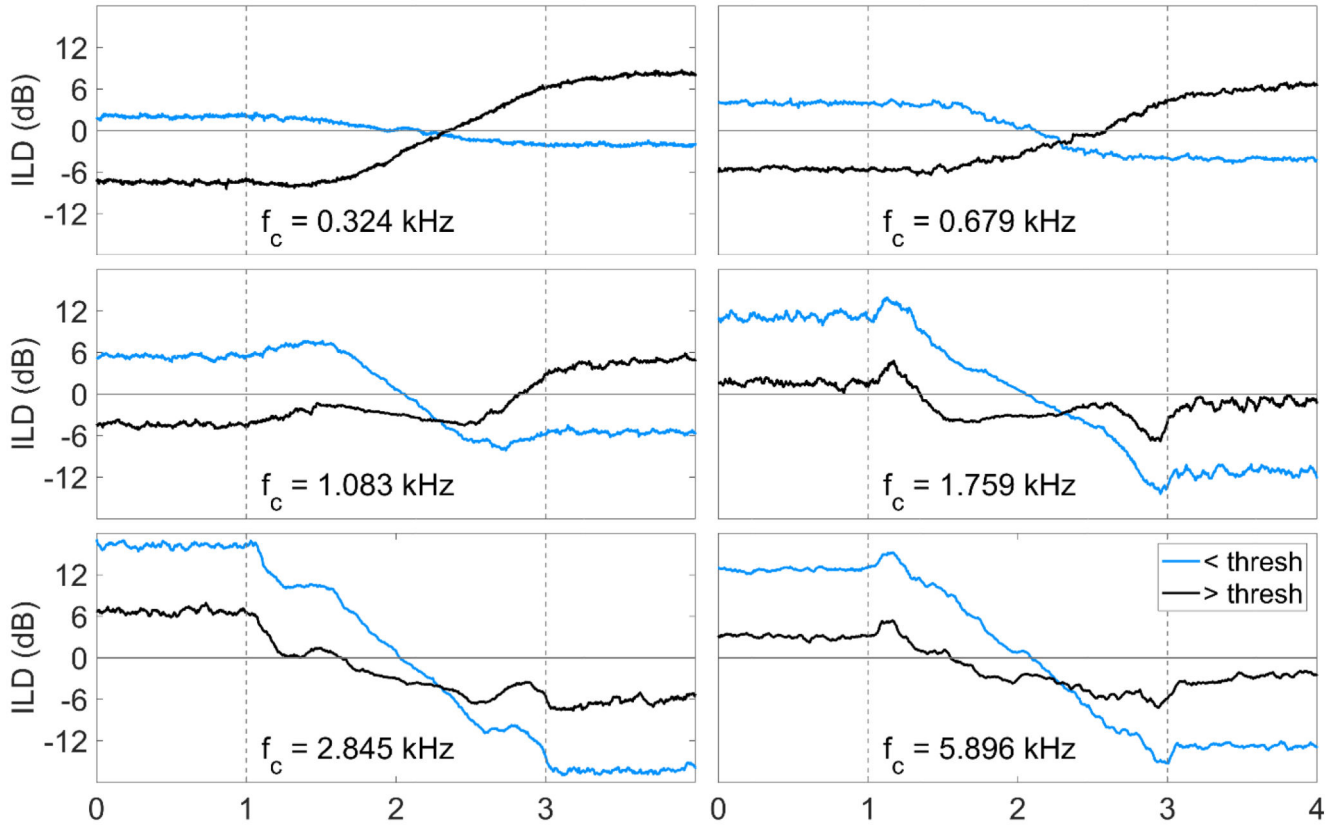

Figure 6.

(color online) Sub- (blue) and supra-threshold (black) ILD plots for 6 channels of a standard map. The input signal was SSN and the head movement was -60° to 60° at 60°s^{-1}, identical to the movement shown in figure 2, middle column. See Table 1 for the bandwidths of each channel. The areas of the plots bounded by the dashed lines show the period of rotational movement.

Europe PMC Funders Author Manuscripts

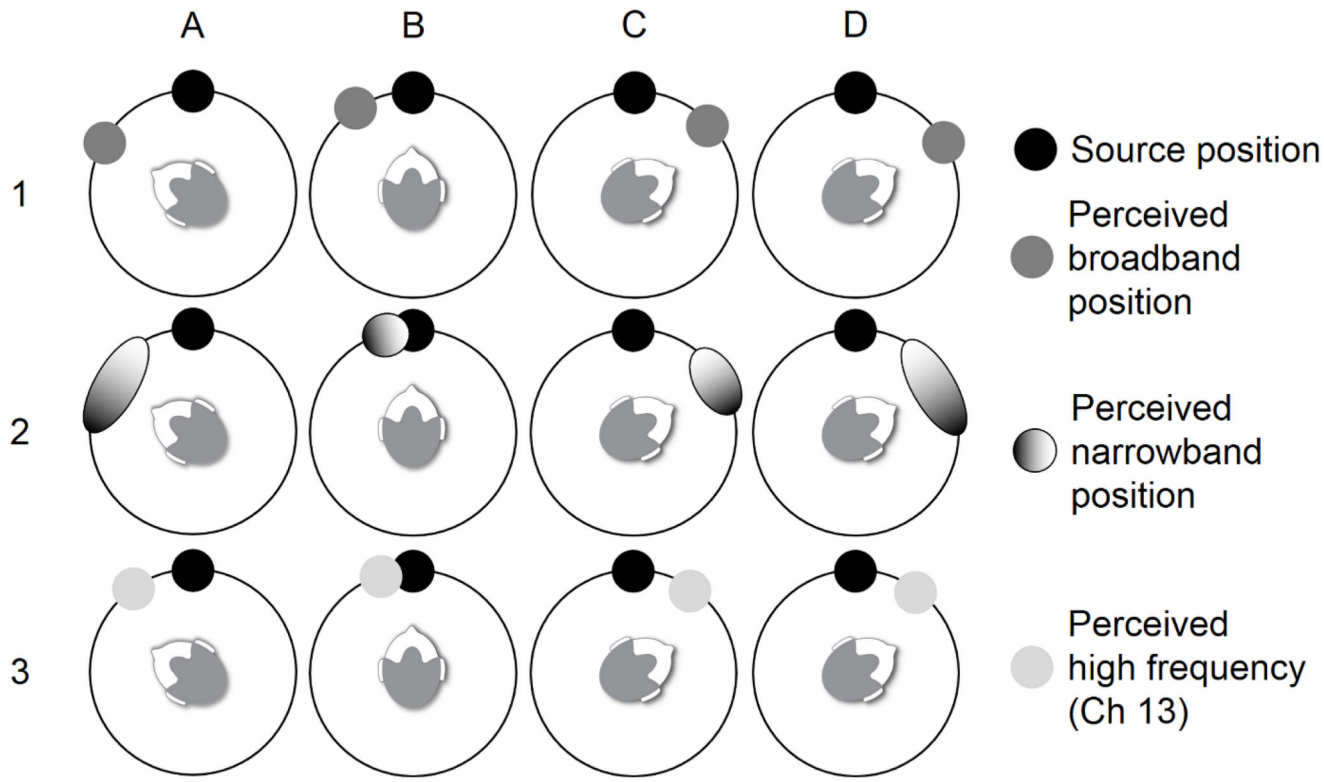

Figure 7.

A schematic of possible perceived source positions at different time points of a -60° to 60° head turn at $60°s^{-1}$. The black circles show the actual source position; the dark grey circles show the possible perceived source position based on the broadband ILD (row 1); the graded ovals show the possible perceived source position based on the channel outputs, darker for low frequency, lighter for high frequency (row 2); the light grey circles show the possible perceived source position based on the output of channel 13, a high-frequency channel (row 3). In column A the head is at -60° and about to move; in column B the head is at 0°, halfway through the movement; in column C the head is at 60° at the end of the movement; in column D the head is at 60° >0.5 seconds after movement has stopped.

Europe PMC Funders Author Manuscripts

Table I

The channel cutoff frequencies used in the simulation

Channel	Low cutoff (Hz)	High cutoff (Hz)	Bandwidth (Hz)
1	238	442	204
2	442	510	68
3	510	646	136
4	646	714	68
5	714	850	136
6	850	986	136
7	986	1189	203
8	1189	1393	204
9	1393	1597	204
10	1597	1937	340
11	1937	2277	340
12	2277	2617	340
13	2617	3093	476
14	3093	3704	611
15	3704	4316	612
16	4316	8054	3738